Multipolymer Interactions in Bulk Heterojunction Photovoltaic Devices

Grant Olson • Senior Project • Cal Poly, San Luis Obispo • June 25, 2012

Multipolymer Interactions in Bulk Heterojunction Photovoltaic Devices

Grant Olson • Senior Project • Cal Poly, San Luis Obispo • June 25, 2012

Abstract

Multipolymer photovoltaics, single layer devices made up of multiple photoactive polymers, can create organic photovoltaics (OPVs) with a wider spectral response than single polymer systems without the difficult fabrication of a tandem. Our group has successfully created multipolymer solar devices with 2% power conversion efficiency. We have analyzed the optical and electrical properties of these devices, and found that it may be possible for polymers to assist each other with charge extraction, though combining polymers disrupts single polymer crystallinity.

Introduction and Background.

Organic solar, a carbon based technology, is an exciting area of research in the development of renewable energy. The technology has the potential to create photovoltaic energy generation systems that have a lower cost per watt than conventional silicon systems, or even fossil fuels.[1] The 580TW of available solar energy dwarfs the projected energy needs of the human race of 16.9TW by 2030, making harnessing it an attractive possibility.[2] Solar energy is virtually free once the installations are in place, and the availability of solar energy is enormous, so it would seem that the low cost option of organic solar would make it a naturally widespread technology. Unfortunately, neither efficiency nor device lifetime are high enough to make a commercially viable organic solar device. Our group's research is focused on improving the efficiency of organic solar cells.

The polymer nature of organic photovoltaics (OPVs) causes the active layers of plastic solar cells to degrade in the presence oxygen, water, and ultraviolet light. As such, maintaining device performance over a reasonable lifetime is a challenge that is still being investigated. For OPVs to be accepted by the market, a combination of increased lifetime and efficiency will be required.[3] A commercial silicon solar panel will convert light into electricity with an efficiency in the range of 15-20%. Currently, the best

verified organic system is a tandem device designed by Heliatek with a power conversion efficiency of 10.7%.[4] The advancements in the field have moved organics towards a working product, but the technology is not yet ready for widespread use.

When creating photovoltaics, the spectrum of light that a cell absorbs plays a large role in the efficiencies that are possible. A material that absorbs a wide range of the solar spectrum will capture more photons, but each photon can only free a single electron, unless it's an exotic material called a multiple exciton generator.[5] The voltage of the cell is determined by the interaction between the energy levels of the active layer and the electrodes, so the cell is ultimately limited in the amount of energy that can be extracted from each photon. This means that the energy of shorter wavelength (higher energy) light will be wasted on such a cell; any energy above the band difference will be lost as heat. It is possible to create a tandem system, like in the record breaking device from Heliatek, which consists of stacking devices on top of each other to give better spectral response.[6] This allows each layer to work at different device voltages, so higher energy photons can contribute more of their energy. Unfortunately, high performance tandems require the currents from each layer to be matched, which makes them more difficult to design and produce, and they lose performance when they are put under a spectra that they are not designed for.[7] What would be ideal is a system that has the broad absorption capability of a tandem, with the ease of fabrication of a single layer device. The multipolymer bulk heterojunction system has the potential to realize both of these goals by combining multiple photovoltaic polymers with synergistic optical and electrical properties to make a well performing hybrid device.[8] In this paper we will explain our methods and results in characterizing our multipolymer system via optical and electrical testing.

Theory

A bulk heterojunction solar cell is so named because the volume between the electrodes is made up of an interpenetrating layer of dissimilar materials. One of these materials is a polymer, P3HT [poly(3-hexylthiophene)] or PCPDTBT [poly[2,6-(4,4-bis-

(2-ethyl- hexyl)-4H-cyclopenta[2,1-b;3,4-b0]dithiophene)-alt-4,7-(2,1,3-benzo-thiadiazole)]], which serves as an electron donor to the other material, a fullerene derivative called $PC_{60}BM$ [[6,6]-phenyl-C61-butyric acid methyl ester]. PCPDTBT is also commonly referred to as ZZ50, named after inventor Zhengguo Zhu achieving success on his 50th try . A fullerene is effectively a bucky ball, 60 carbon atoms arranged in a spherical shape with a tail added to the structure to improve solubility, and is used as our electron acceptor. Classical devices (made of a single polymer and PCBM) have a single bulk heterojunction layer made of a blend of polymer and PCBM, so they are relatively easy to fabricate, see Figure (1).[9] Tandem devices have multiple polymer layers, with intermediate electrodes separating them. To minimize losses, all active layers of a tandem must be tuned to have the same current output.[10] This increases the complexity in design and fabrication of devices, driving up the potential cost. Additionally, because each layer absorbs in a different region of the spectra, devices that are designed to absorb solar light will not convert other light sources efficiently. Our proposed design, the multipolymer bulk heterojunction device, does not require current matching or an intermediate electrode, eliminating the most difficult and costly aspects of design and fabrication of tandems.[11]

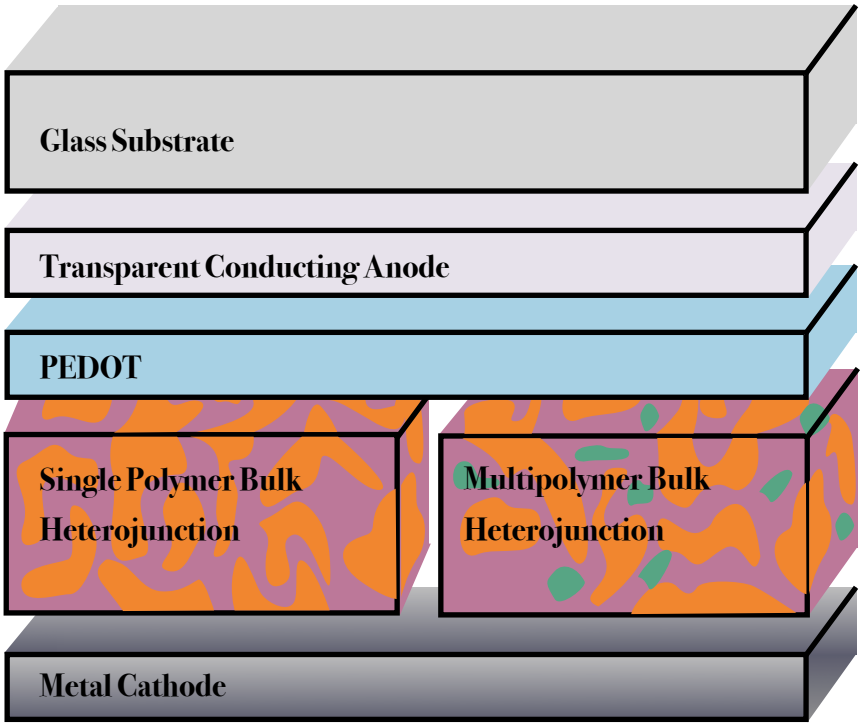

Figure (1) - Single polymer (left) and multipolymer (right) bulk heterojunction device layers

The mechanics of an OPV begins with the interaction of a photon with the polymer in our bulk heterojunction layer, see Figures (2) and (3). When a photon of sufficient energy is absorbed by the polymer layer it excites an electron from the Highest Occupied Molecular Orbital (HOMO) to the Lowest Unoccupied Molecular Orbital (LUMO). The space that the electron previously held is now empty, creating a region of relative positive charge that we call a hole. The now excited electron and hole are bound together into an exciton, and the pair are free to travel for a brief period before they recombine and lose their energy. The exciton's lifetime is about 100ps, during which time it can diffuse about 10nm.[12] If it happens to encounter an interface between the polymer and the

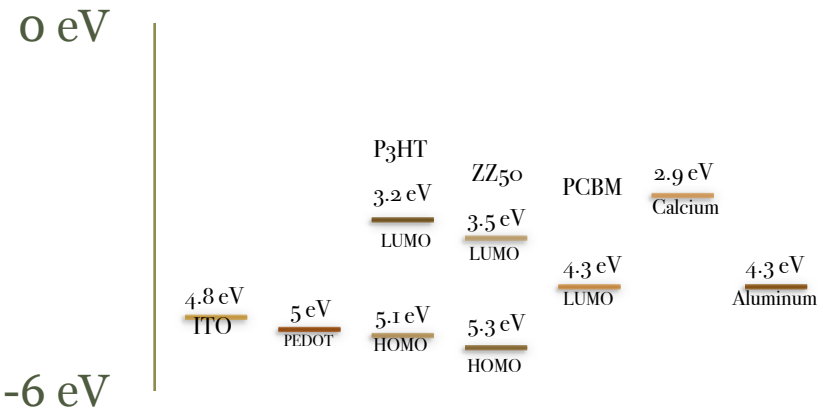

Figure (2) - Energy levels of the device layers

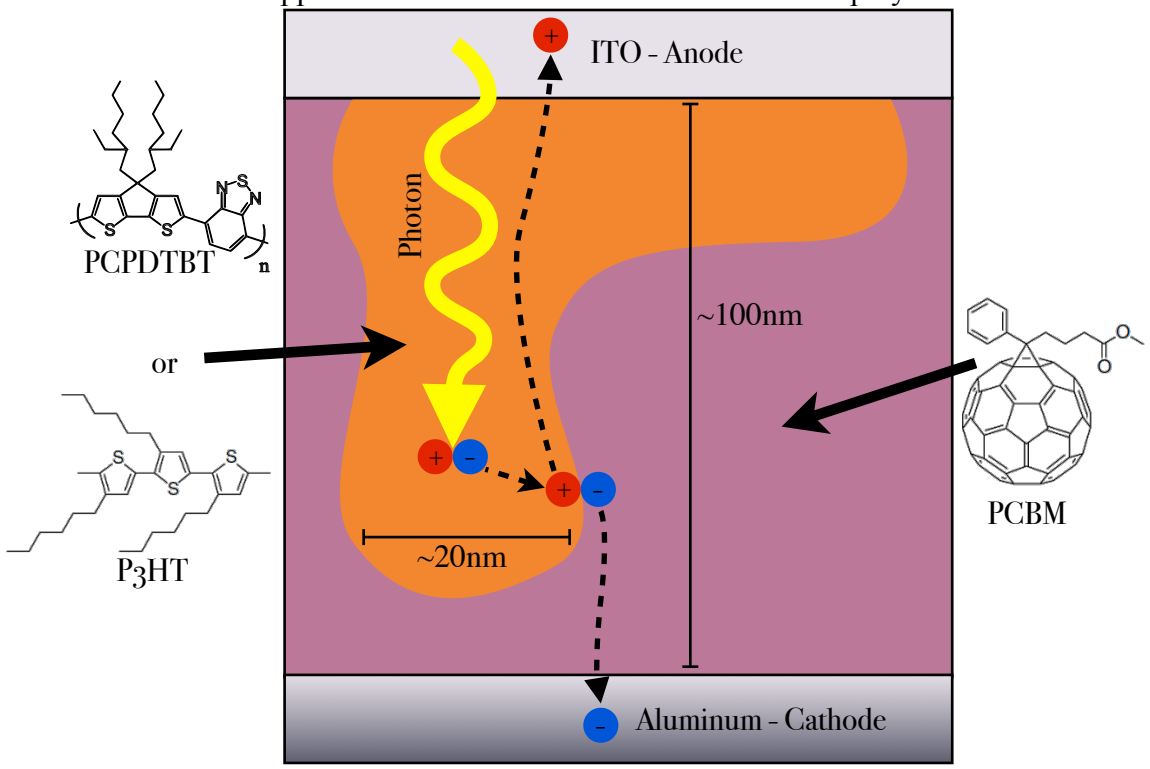

Figure (3) - Exciton generation in the bulk heterojunction layer

PCBM before recombining the large electronegativity of the PCBM will pull the hole and the electron apart.[13] The two charges are then free to travel along their charge pathways (the hole along the polymer, the electron along the PCBM) to their respective electrodes, assuming that both charges have a continuous path to the electrode. Consequently, polymer region size is an important factor in device performance, because devices with too large of regions will not be able to split excitons that are generated far from the heterojunction. Additionally, devices with excessively small regions will not have enough continuous pathways to extract charge after the excitons have been split. Exciton lifetime gives them a travel distance of around 10nm, as stated before, so an ideal region size would be on the order of 20nm, so that no excitons are lost to recombination and a maximum number of pathways exist to extract charge from the device, see Figure (3).

The driving force behind the migration of each charge to their respective electrode is the electric field created by the work function difference between the cathode (Calcium:Aluminum) and the anode (Indium Tin Oxide) as shown in Figure (2), see equation [1], where F is the force exerted on the electron, q is the electron charge, E is the strength of the electric field, d is the distance between the electrodes and Φ is the work function of the cathode (c) and anode (a).

$$F = q\mathrm{E} = q\frac{\left(\Phi_c - \Phi_a\right)}{d} \qquad [1]$$

The PEDOT (Poly(3,4-ethylenedioxythiophene) poly(styrenesulfonate)) layer (a conducting layer of polymer) and the calcium layer serve a similar purpose in their inclusions in our devices, because they have energy levels that are slightly lower (in the case of PEDOT) or significantly higher (in the case of calcium) than the ITO or aluminum respectively. These materials serve to pin our two electrodes at larger voltages and thus create a larger electric field in our devices, increasing the force on extracted charges. The energy level difference between the HOMO of the polymer and the LUMO of the PCBM is a theoretical maximum for our polymer device's open circuit voltage. A tuning of the energy levels to more closely align the polymer and PCBM LUMO levels will decrease the thermalization losses when the exciton separates.[14] Unfortunately, such

a change will decrease the tendency of excitons to dissociate, since the difference between the LUMO of the polymer and the LUMO of the PCBM serves as a driving force to separate excitons. Modifying energy levels must be balanced carefully by those groups that actively modify their polymers.[15]

Testing a device's optical and electrical properties can help probe internal morphology. The most basic electrical testing is done by measuring current output while devices are illuminated and subjected to a voltage bias, so that we can simulate different loading conditions to find each device's max power point. Device tests are analyzed to extract the open circuit voltage (V_{oc}), short circuit current density (J_{sc}), and maximum power conversion (P_{max}), see Figure (4). To find device efficiency it is necessary to know the intensity of incident light ($P_{incident}$), from which we use equation [2] to calculate the power conversion efficiency.

$$\eta = \frac{P_{\max}}{P_{incident}} \qquad [2]$$

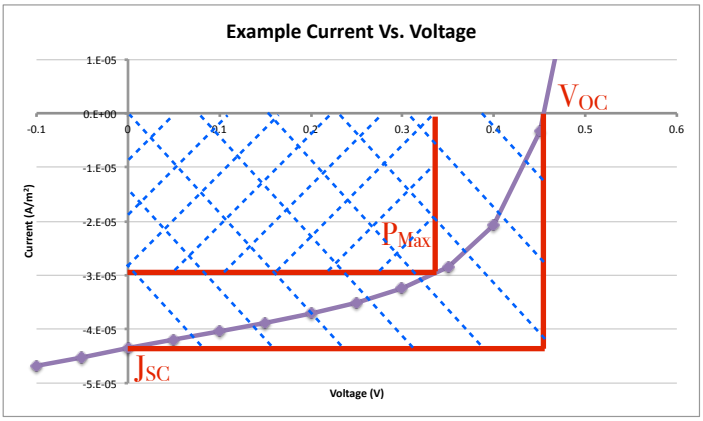

Figure (4) - Example JV testing curve with open circuit voltage, short circuit current and max power labelled. Fill factor is the ratio between the area shaded top-right to bottom left and the area shaded top left to bottom right

Fill factor is a relationship between the maximum power extracted from a device and the open circuit voltage multiplied by the short circuit current, as shown in equation [3]. It is also the ratio between the area of P_{max} and the area enclosed by V_{oc} and J_{sc} Fill factor is often indicative of a device's ability to extract charge, because a good fill factor implies that excitons are able to dissociate and able to travel to their electrodes even when the internal electric field is weakened by a voltage bias.

$$FF = \frac{P_{\max}}{(J_{sc})(V_{oc})} \qquad [3]$$

A low J_{sc} can indicate that the polymer regions in the device are too small, creating trapping regions that are not connected to electrodes, or too large, making excitons that do not reach the heterojunction before recombining. Current is also related to device thickness, and can be negatively impacted if the active layer is too thin (the device will not absorb very much light) or too thick (the device will not be able to extract much charge) A low V_{oc} can be indicative of shorting pathways between the two electrodes. Fill factor is incredibly sensitive to active layer morphology and device thickness. Efficiency gives an expression of how all the different parts of the device mechanics are working together

A more advanced testing procedure, External Quantum Efficiency (EQE), is a measurement of a device's ability to convert incident photons into extracted electrons as a function of wavelength. We can integrate this data to predict short circuit current values for any spectra. EQEs are taken by exposing a device to a known number of photons at a narrow band of wavelengths and measuring the J_{sc} of the device, then dividing that current by the number of incident photons. This is shown in equation [4], where $J(\lambda)$ is the short circuit current density per wavelength interval, $I(\lambda)$ is the incident light intensity per wavelength interval, λ is the wavelength of light, h is planck's constant and c is the speed of light.

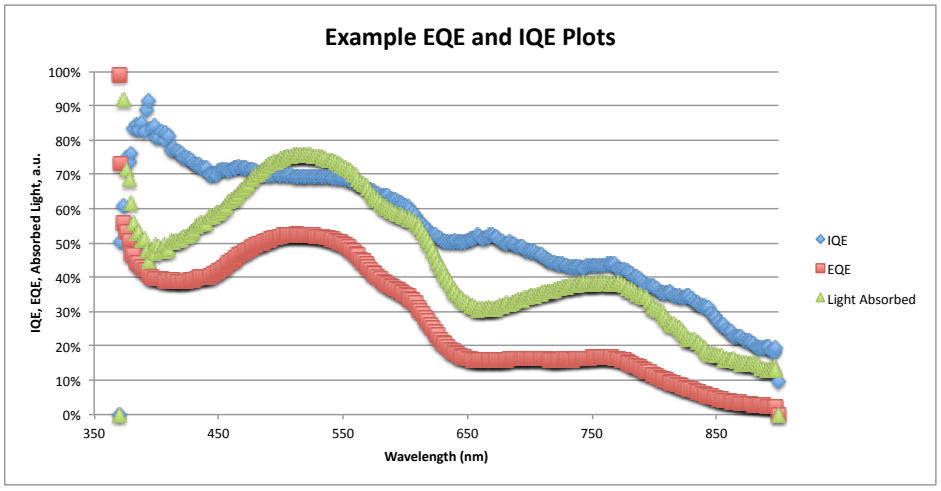

Figure (5) - Example of IQE, EQE and light absorbed

$$EQE(\lambda) = \frac{\left(\frac{J(\lambda)}{e}\right)}{\left(\frac{I(\lambda)\cdot\lambda}{hc}\right)} \qquad [4]$$

If we combine this data with an optical density measurement of the device, which characterizes the absorption of the cell, we can create an IQE plot, see Figure (5), the equation for which is shown in [5], where α is the optical density of the device and R is the reflectivity of the rear electrode. IQE is a ratio of the number of electrons extracted to the number of photons absorbed, and this data can provide insight into device characteristics.

$$IQE(\lambda) = \frac{\left(\frac{J(\lambda)}{e}\right)}{\left(\frac{I(\lambda)\cdot\lambda}{hc}\right)\cdot\left(1\text{-}10^{-\alpha\cdot(1+R)}\right)} \qquad [5]$$

One hypothesis for the internal mechanics of a multipolymer system is that P3HT will be able to help ZZ50 with charge extraction because it is energetically favorable for holes in ZZ50 to diffuse into P3HT due to P3HT's higher HOMO level. If this is correct, the IQE values of ZZ50 in a multipolymer blend would be higher that the IQE values of ZZ50 alone, because holes traveling in the ZZ50 are able to use P3HT channels to reach the ITO after they have dissociated.

Optical analysis of polymer layers also yields some data about the internal structure of devices. The crystallinity of a polymer can be shown in the optical signature that it creates, such as the increased absorption and "anneal bump" shown in Figure (6) when P3HT is annealed.[17] Optical density is related to the light transmitted after a single pass through the device by the relationship shown in equation [6], where I_{trans} is the light transmitted, I_0 is the incident light and α is the optical density.

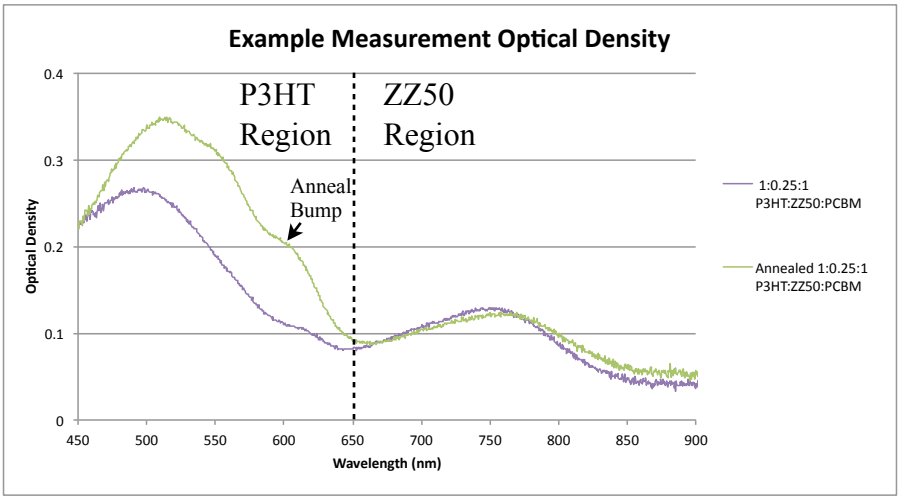

Figure (6) - Example of optical density measurement

$$I_{tran} = I_0 \cdot 10^{-\alpha} \qquad [6]$$

Optical data is particularly important in the case of multipolymer blends, because the interactions between different photovoltaic polymers in a single layer is not well documented. If the absorption of a particular polymer in the device is significantly lower than it should be based on concentration, then we argue that the other polymer may be interrupting the crystallinity, which can negatively impact the absorption. This is confirmed if we see a larger than normal rise in optical density when we subject the device to thermal anneal because the P3HT, which tends to increase in region size and crystallinity when annealed, was less crystalline when the device was first fabricated.[17] In addition to plotting the optical density data, our group uses a matlab tool to approximate the optical density data of a multipolymer device by summing the optical density data of the two separate polymers using a method of least squares. This allows us to measure the optical density of each polymer in a blend, and to assign numerical values to the optical strength of each polymer. An example of the summing process is shown in Figure (7), and the analysis of this plot reveals that the P3HT signature of the blend is 0.68 and the ZZ50 signature is 0.36. This means that the blended devices optical signature is most closely approximated by adding the P3HT control multiplied by 0.68 to the ZZ50 control multiplied by 0.36. We can compare these calculated values to the values that we would expect based on solution concentration using equation [7].

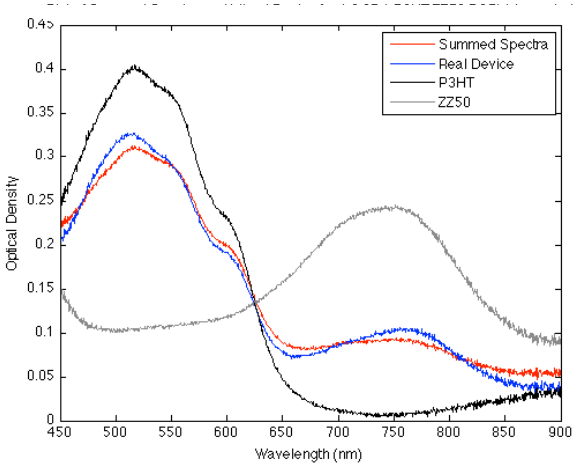

Figure (7) - Example Matlab analysis of multipolymer spectra. Black and grey lines are the control spectra of P3HT and ZZ50, the blue line is the actual multipolymer optical density, and the red line is the best approximation made by summing the controls

$$(\alpha_{P3HT\ \text{expected in blend}}) = (\alpha_{P3HT\ control})\frac{(mass\ fraction\ P3HT\ in\ blend)}{(mass\ fraction\ P3HT\ in\ control)} \qquad [7]$$

In the example, the control device was made with a 20:20 mg/ml P3HT:PCBM solution, so the control mass fraction is 0.50, and the blend was made of 16:4:16 mg/ml

P3HT:ZZ50:PCBM solution, so the P3HT mass fraction is 0.44. Since the P3HT optical density of the control is defined as 1, we would expect the P3HT signature of the blend to be around 0.88. It's quite a bit lower than that, at 0.68, and we will discuss the repercussions of that the analysis section.

Experimental

All experimental solar cell devices are fabricated in the Cal Poly San Luis Obispo's Polymer Lab, and follow essentially identical manufacturing steps. Devices are created in an inverted fashion; we begin with the glass substrate and transparent electrode (what will become the top of the device) and create the other layers on top of those two. The structure of our devices is shown in Figure (8), and the steps for manufacturing can be thought of as progressing from top to bottom in Figure (1).

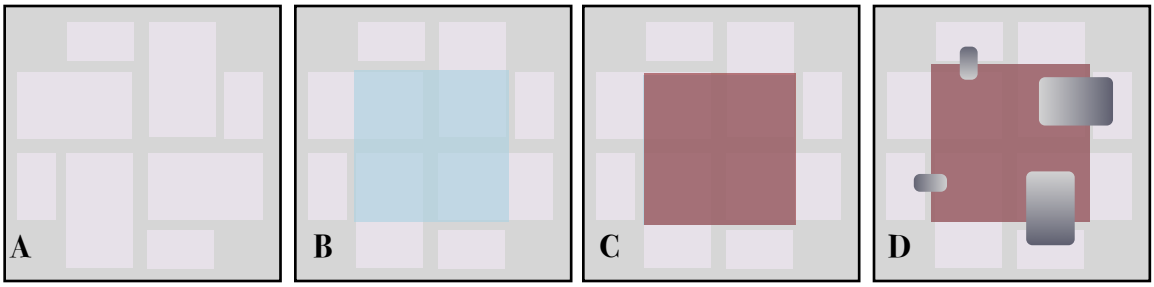

Figure (8) - Device fabrication steps; (A) Begin with a glass substrate with ITO stencilled (B) Spin coat and wipe a layer of PEDOT, anneal (C) Spin coat and wipe a layer of polymer solution, anneal (D) Evaporate electrodes

We begin with a glass substrate that has been pre-stenciled with ITO (Indium Tin Oxide), in the shape shown by Figure (8A). Each quarter of the device will be turned into a single pixel for testing after fabrication is complete as shown in Figure (8D). ITO is a transparent conductor (~50nm thick), and will act as the anode in our devices. The substrates with the ITO are visually inspected for faults or dirt then subjected to ultrasonication for 3 minutes in a bath of acetone, then again in isopropanol to remove any contaminations. Substrates are then transported under flow of nitrogen to a UV ozone machine. Here they are subjected to ultraviolet light and ozone for at least 30 minutes to further clean the substrates.

Devices are spin coated with PEDOT at 5k rpm for 60 seconds, then the outer pads are wiped to prevent shorting pathways between the inner and outer electrodes, see Figure (8B) . PEDOT is not necessary to create a working device, but the addition of this layer increases output voltage as discussed above. The PEDOT application step takes place in a dust free area in standard atmosphere. After wiping the PEDOT off the outer layers of ITO the devices are subjected to a thermal anneal at 140˚C for 10 minutes to remove any excess water. While the devices are still hot they are loaded into an antechamber and transported into the glovebox to minimize water contamination. The glovebox is a pure nitrogen atmosphere where water and oxygen particles are usually kept to less than 1 part per million, to protect the polymers from degradation.

Polymer solutions are typically created 24 hours in advance, using a precision scale to weigh the polymer and fullerene solutes before adding them to a mixing bottle. After adding the solvent we allow the solution to mix on a hot plate at 50˚C with a magnetic stir bar rotating at 500 rpm. The polymers used are P3HT and ZZ50 with PCBM fullerene, and typical solvents are chlorobenzene (CB) and dicholorobenzene (DCB). After being allowed to mix, the active layer of our devices is applied using a spin coater, with spin speeds ranging between 600-5000 rpm (with higher speeds creating thinner devices). After spin coating the polymer layer, devices have their outer ITO pads wiped using a THF swab, see Figure (8C), so that our cathode can contact the small ITO pad which will serve as our connection point for electrical testing. THF has a low boiling point (66˚C), which makes it evaporate quickly after wiping. The fast evaporation means that the solvent will not drip or run, allowing for a carefully controlled wipe. Devices are then labeled with the device ID and run ID, and then may be subjected to a pre-cathode anneal before being transported into the solvent free glove box for cathode application.

Devices are transported through a second antechamber into a cleaner nitrogen atmosphere, one without solvent, to continue the fabrication process. A metal evaporator, encased in a bell jar that can be evacuated by a diffusion pump to ~$1x10^{-6}$Torr, is used to apply a double Ca:Al electrode that finishes the devices. The electrodes are stenciled out as shown in Figure (8D) creating two large pixels with active areas of $42mm^2$ and two

small pixels with active areas of 3.75mm^2. The active area of a device is the place where all layers overlap. The first electrode is a 20nm layer of calcium, which serves the same function as PEDOT on the ITO side of the device. Calcium is extremely reactive, so we cap our devices with another 80nm of aluminum. Aluminum provides high conductivity, and after forming its initial oxide layer does not corrode, so it helps to protect the calcium after evaporation. After the application of these two metals, the device is complete and ready for testing.

The testing process begins inside the solvent free box with a Dolan Jenner light sources illuminating the testing jig where the devices are held. The devices are subjected to a light intensity of 18W/m^2 while run through a series of devices voltages using a Keithley voltage source. This process is controlled by labview, which also records the current as is sweeps in 0.05V increments from -1V to +1V. Devices are also optically tested inside the solvent free box using an Ocean Optics lamp and spectrometer. Absorption data is taken for the devices using a substrate with ITO and PEDOT as the light baseline. After initial electrical (JV) and optical testing, devices may be subjected to anneal treatments and tested again.

Once we complete preliminary testing, devices are selected to be packaged and removed from the glove box for testing under true solar conditions. Devices are transported via antechamber to the solvent box where a layer of aluminum tape is applied to the bottom of the device (the side with the metal cathode on it). The added aluminum tape serves to limit the amount of oxygen that can diffuse into the device and degrade the polymer layer and calcium electrode. Taped devices are then transported out of the box via antechamber and sealed with epoxy to form an additional protective layer. Solar testing takes place immediately after packaging is completed (industry standard is to test under AM 1.5, or the sun's light as it passes through 1.5 atmospheres, which occurs when the sun is 48˚ off of azimuth). The final form of testing then occurs in our optics lab, where light from a Dolan Jenner source is sent through a monochromator and then onto our device while we measure the short circuit currents. This measurement gives us the external quantum efficiency (EQE) as discussed in equation (4)

Device run B was designed to test the effectiveness of a polymer solution with equal parts P3HT and ZZ50, and the following device parameters were used. The solution for application of the polymer was created as a 8:8:24mg/ml P3HT:ZZ50:PCBM mixture in chlorobenzene. Polymer was applied at 2k, 4k and 5k rpm spin speeds, with the breakdown of devices shown in Table (1). After the cathode was applied (20nm calcium, 70nm aluminum) devices were subjected to optical and electrical testing (discussed in analysis), and some devices were selected for extensive anneal testing, as shown in Table (1).

Device #	Spin Speed	Precathode Anneal	1-16-12 Anneal	1-18-12 Anneal	1-19-12 Anneal	1-24-12 Anneal	2-28-12 Anneal	4-3-12
1	2k rpm		105/10	105/20 +130/10	130/10 +150/10	150/10		
2	2k rpm							
3	2k rpm							
4	4k rpm	105C/10min					150/10	
5	4k rpm	105C/10min				150/10		
6	4k rpm	105C/10min						
7	4k rpm						150/10	
8	4k rpm		105/10	105/20 +130/10	130/10 +150/10	150/10		
9	4k rpm							140/30
10	5k rpm							
11	5k rpm						150/10	
12	5k rpm		105/10	105/20 +130/10	130/10 +150/10	150/10		

Table (1) - Device run B (1:1:3 P3HT:ZZ50:PCBM) fabrication and anneal data

Device run C was designed to test the effectiveness of small concentrations of ZZ50 being added into more conventional P3HT:PCBM devices. The solutions created were made as 16:4:16mg/ml P3HT:ZZ50:PCBM (devices 1-4), 8:32mg/ml ZZ50:PCBM (5-8), and 20:20mg/ml P3HT:PCBM (9-12). The PEDOT layer on this run was not wiped, resulting in devices with higher current leakages than usual, and the devices were

given 100nm of aluminum as a cathode; no calcium was applied. The first two devices in each group were subjected to a thermal anneal for 10 minutes at 105˚C, then all devices were tested electrically and optically. Devices 1, 2, 9, and 10 were removed from the glovebox for AM1.5 and EQE testing.

Analysis

Analysis of devices begins with electrical testing in a low light environment. Figure (9) shows the testing results of a single pixel from a P3HT:PCBM (referred to as P3HT) control device, a ZZ50:PCBM (referred to as ZZ50) control device, and P3HT:ZZ50:PCBM blends from runs B and C. Of the pure polymer devices, P3HT has a better fill factor, most likely due to it's crystallinity, resulting in higher power conversion efficiencies, while ZZ50 creates higher open circuit voltages and short circuit currents. The plot shows that the 1:1:3 P3HT:ZZ50:PCBM blend (referred to as 1:1:3) from run B has an open circuit voltage that matches P3HT, but a short circuit current density that is lower than either of the pure polymers. The 1:0.25:1 blend from run C has a short circuit current density that matches P3HT, with a higher open circuit voltage. We conclude that adding ZZ50 can increase the voltage of P3HT devices, although increasing the concentration of ZZ50 too much can reduce charge extraction.

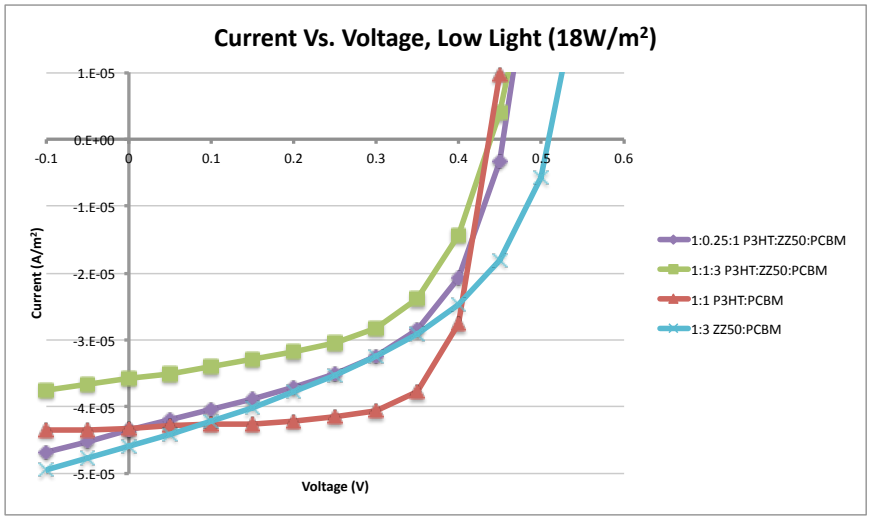

Figure (9) - JV Curves of Various Devices

This conclusion is supported by optical analysis of the blends when compared to the pure polymer devices. A simple plot of optical density is shown in Figure (10), where the bolded lines show "pure" P3HT and ZZ50 devices. The thinner lines show two

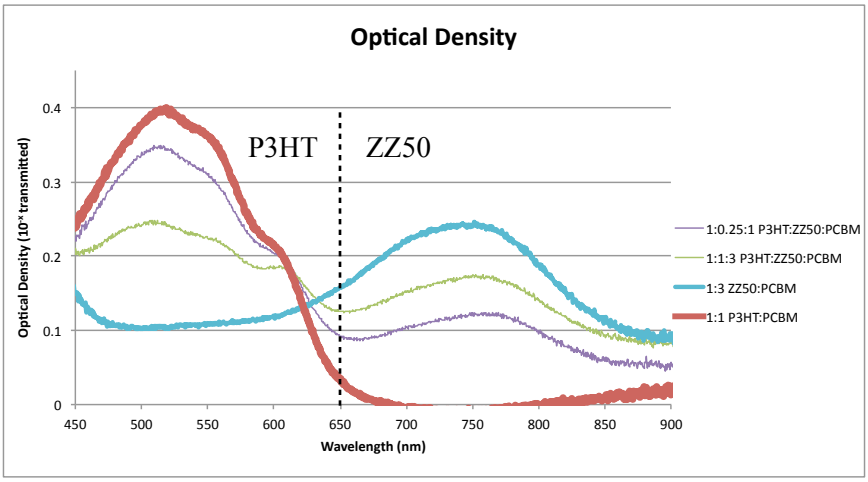

Figure (10) - Optical density plots of of various devices. Thick lines are single polymer devices, thin lines are multipolymers

P3HT:ZZ50:PCBM blends with different polymer ratios. The green line is a polymer solution that is made of equal parts P3HT and ZZ50, which is expressed in its lower peak in the P3HT region and greater absorption in the ZZ50 region. Similarly, the purple line is a blend with a much lower ZZ50 concentration, so it absorbs significantly more light at shorter wavelengths than at longer wavelengths. Figure (11) shows a single device, subjected to many stages of thermal anneal, that was optically tested after each heat treatment. The ZZ50 portion of this device diminishes over time and with anneals, while the P3HT portion increases with both time and thermal anneal

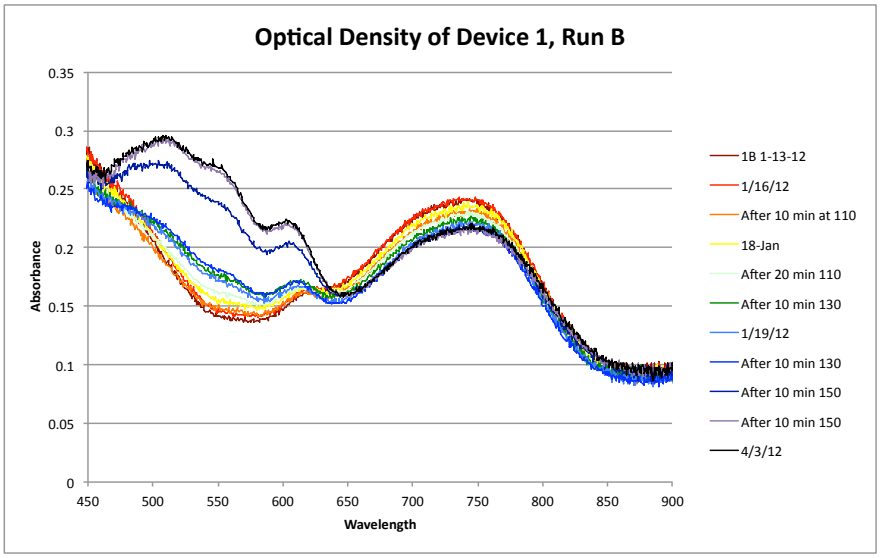

Figure (11) - Change in optical density of a 1:1:3 P3HT:ZZ50:PCBM blend with anneal

Using the matlab tool explained in the theory section, we separate the optical density measurements of the 1:0.25:1 and 1:1:3 blends into component spectra before and after they have been annealed, see Figure (12). The signature values extracted from the tool are shown in Table (2), where each value is the strength of that polymer's optical density compared to the control's optical density. The control spectra for the devices that have not been

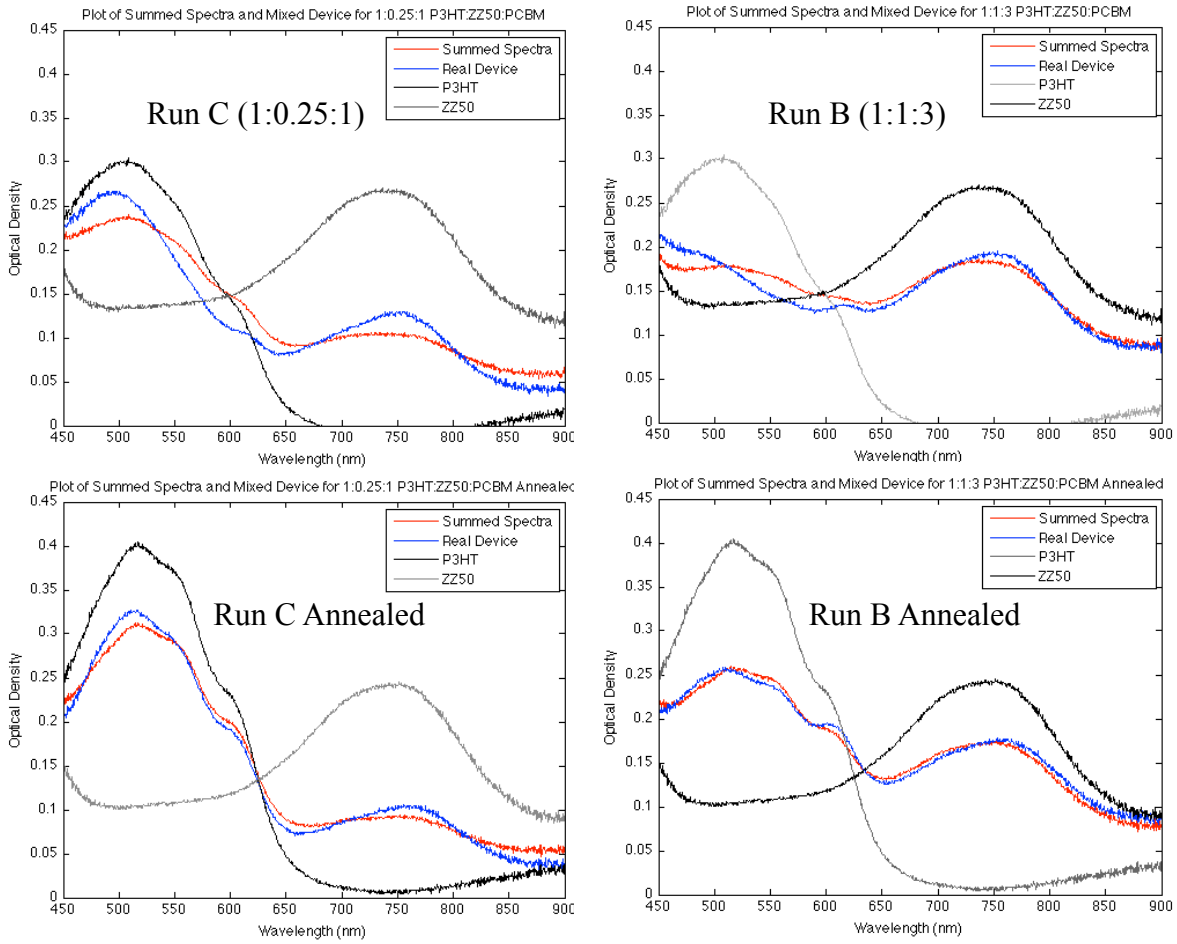

Figure (12) - Matlab analysis of 1:0.25:1 and 1:1:3 blends before and after anneal

annealed are also not annealed, and the control spectra for the annealed devices have been subjected to an anneal at 105˚C for 10 minutes. The rises and drops in the optical density spectra can be seen in Figure (13), which shows the striking increase in the strength of P3HT's absorption region (<650nm) and the slight if at all decrease of ZZ50's absorption region (>650nm) with thermal annealing. By inspection, we note that annealing tends to increase the absorption of blended devices in the P3HT region, and diminish their absorption in the ZZ50 region.

Absorption Coefficients of Different Devices	P3HT Signature	ZZ50 Signature
1:0.25:1 P3HT:ZZ50:PCBM	0.60	0.42
1:0.25:1 P3HT:ZZ50:PCBM Annealed	0.68	0.36
1:1:3 P3HT:ZZ50:PCBM	0.28	0.70
1:1:3 P3HT:ZZ50:PCBM Annealed	0.46	0.70

Table (2) - Optical signature values corresponding to Figure (12)

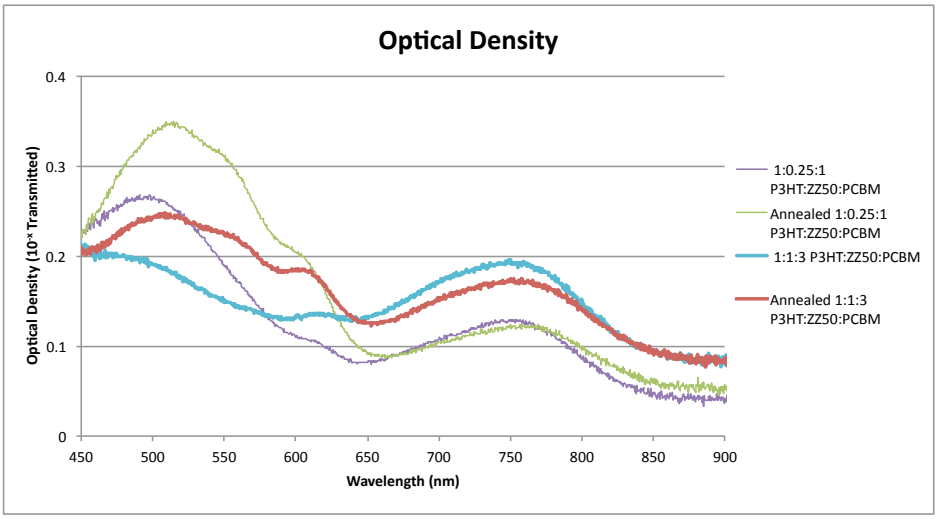

Figure (13) - Stacked optical density plot of blends before and after they have been annealed. Thick lines are 1:1:3 P3HT:ZZ50:PCBM, thin lines are 1:0.25:1 P3HT:ZZ50:PCBM

Using the values in table (2), we found that blends with larger ZZ50 concentrations that were subjected to thermal anneal were capable of larger rises in the P3HT region of the optical density than blends with lower concentrations. The proportionality between ZZ50 concentration and anneal effectiveness does not apply to the ZZ50 region of the optical density. Pure ZZ50 devices do not respond favorably to thermal anneals, and the ZZ50 portion of a multipolymer system is no different.

When we apply the data in table (2) to equation [7], along with the mass fractions from the experimental section, we get the percentages of expected values in table (3). Note that ZZ50, regardless of concentration or anneal, tends to have an optical density that is within 10-20% of the expected value based on mass fraction. This, coupled with the lack of change in ZZ50's optical signature with thermal anneal, implies that ZZ50 regions are not significantly impacted when the material is placed in a multipolymer system. P3HT, on the other hand, has a depressed optical signature when placed in a multipolymer blend. When this information is combined with the observation that the P3HT signatures of the annealed devices are higher than they are

Ratios of Expected Absorption to Actual	% of expected P3HT signature	% of expected ZZ50 signature
1:0.25:1 P3HT:ZZ50:PCBM	68%	95%
1:0.25:1 P3HT:ZZ50:PCBM Annealed	76%	81%
1:1:3 P3HT:ZZ50:PCBM	70%	86%
1:1:3 P3HT:ZZ50:PCBM Annealed	115%	86%

Table (3) - Ratio of extracted optical densities to anticipated values based on mass fraction of solution

in unannealed blends, we claim that the crystallinity of P3HT is negatively impacted when it is used in a multipolymer blend, but that this crystallinity can be made with thermal anneal. Note that in this table the 1:1:3 device was subjected to a much more extensive anneal regimen than the control group or the 1:0.25:1 blend, which is the reason for its extreme rise after thermal anneal.

Since ZZ50 has little response to thermal anneal and the response of P3HT is significant, it would make sense that devices with higher ZZ50 concentrations would require more intense thermal treatments to experience changes in device performance. This hypothesis is supported by the efficiency data taken for runs B and C. Figure (14) shows the efficiencies of an annealed and unannealed device from run B over a wide range of time and anneals. When this data is compared with Figure (15), which has an annealed and unannealed device from run C, we note that when the blend from run B was subjected to an anneal of 110˚C for 10 minutes (which caused the efficiency of run C to increase by more than an order of magnitude) it experienced no change in performance. It was not until the device was baked for 10 minutes at 130˚C that we began to see a significant rise, and the device did not achieve its maximum

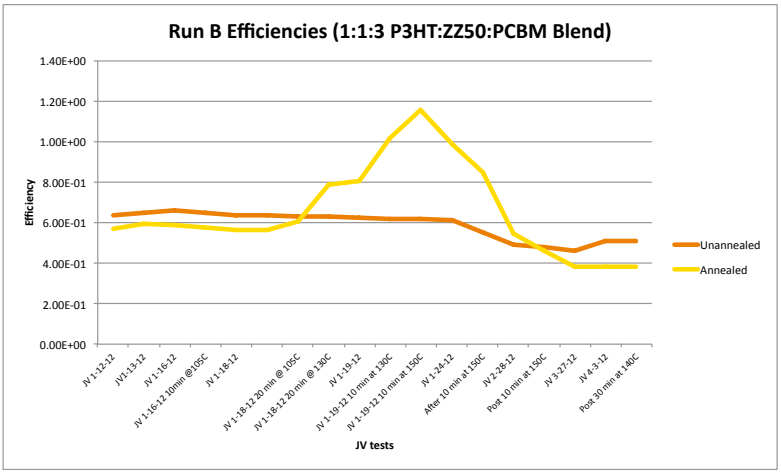

Figure (14) - Efficiency change of 1:1:3 P3HT:ZZ50:PCBM devices with thermal anneal and over time

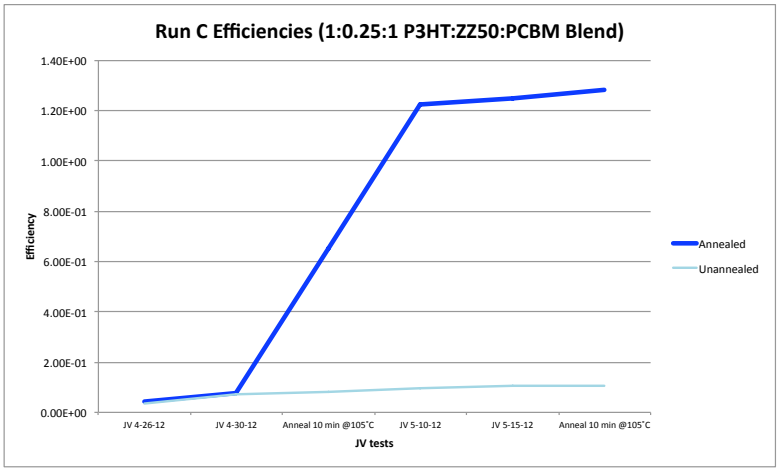

Figure (15) - Efficiencies change of 1:0.25:1 P3HT:ZZ50:PCBM devices with thermal anneal and over time

efficiency until it had been annealed at 150˚C. Previous attempts to anneal pure P3HT devices at temperatures above 130˚C in our lab have resulted in significant losses in performance, so the addition of the ZZ50 is clearly changing the way the devices respond to thermal anneal.

After transporting the devices from both runs out of the glovebox and testing them in solar conditions, the best device from run B registered only 0.9% electrical conversion efficiency. Run C's device converted over 2% of incident light energy to electricity, and the JV curves for both devices are shown in Figure (16). Note that the 1:0.25:1 device reports a higher power conversion efficiency at high light than at low light (from 1.3% to 2.0%), while the efficiency of the 1:1:3 is significantly decreased in high light conditions (from 1.2% to 0.9%). Under ideal conditions a device's efficiency should increase in high intensity situations, because the current scales linearly with light intensity and the voltage increases slightly as the nearest states in the energy levels are evacuated. When a charge extraction problem exists however, the device is incapable of taking advantage of the large number of excitons created, and loses conversion efficiency. This electrical data supports the idea that ZZ50 interrupts P3HT's ability to extract charge effectively when incorporated into a device in high concentrations.

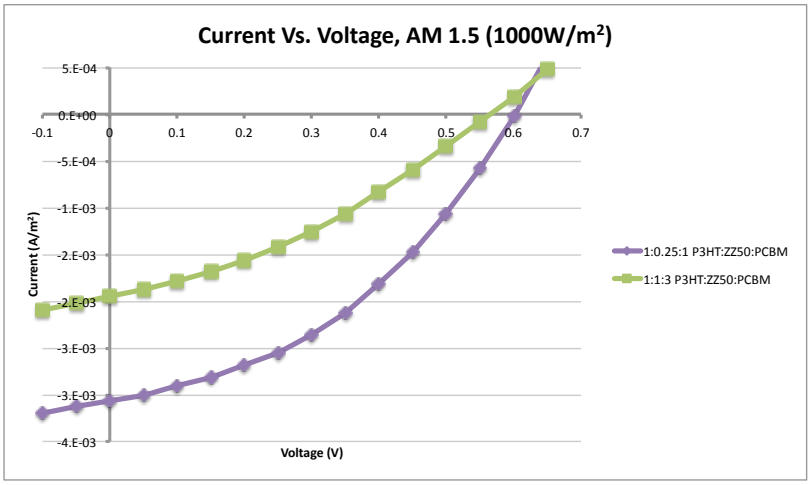

Figure (16) - JV curves of the multipolymer blends under AM 1.5 conditions

The final aspect of testing and analyzing multipolymer solar cells uses IQE to see if the polymers in the active area have the capacity to assist each other with charge extraction. In a system where one polymer is helping another, we would expect a region of the plot to exceed the pure polymer values. Figure (17) shows our IQE data for run C (because IQE is made by dividing an EQE spectra by the percentage of photons absorbed,

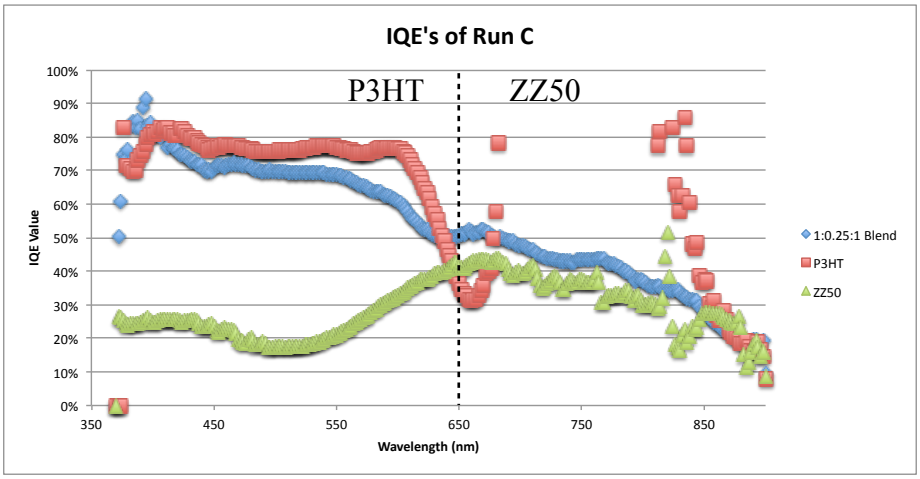

Figure (17) - IQE plots of run C devices

the IQE of P3HT is unreliable above 650nm due to low absorption). The higher blend IQE in the ZZ50 portion of the spectra than pure ZZ50 may imply that P3HT is providing hole extraction pathways to the ITO for excitons made in ZZ50. Further testing is needed to verify this polymer interaction, as the rise is not large enough for testing to be conclusive.

Conclusion

We have used the multipolymer system to make working devices, with power conversion efficiencies as high as 2% in AM 1.5 conditions. Our proposed method of electrical interaction between polymers, with P3HT acting as a hole pathway for ZZ50, seems to agree with our IQE data, although more testing will be needed to verify this conclusion. We have shown that adding ZZ50 to P3HT device disrupts P3HT's crystallinity, and we have found that such interruptions can be overcome with thermal anneals. Further testing should be done on this method of increasing the spectral range of single layer devices to ascertain whether or not multipolymers can result in higher efficiencies than single polymer devices.

References

[1] G. Dennler, M. C. Scharber, and C. J. Brabec, “Polymer-Fullerene Bulk-Heterojunction Solar Cells,” Advanced Materials, **21**, 1323–1338 (2009)

[2] M. Z. Jacobson and M. A. Delucchi, "A path to sustainable energy by 2030," Scientific American **301** (5), 58-65 (2009).

[3] C. H. Peters, et al. “High Efficiency Polymer Solar Cells with Long Operating Lifetimes,” Advanced Energy Materials, **1**, 491-494 (2011)

[4]<http://www.pv-tech.org/news/heliateks_organic_tandem_solar_cell_verified_at_10.7_record_conversion_effi>

[5] R. J. Ellingson, et al. “Highly Efficient Multiple Exciton Generation in Colloidal PbSe and PbS Quantum Dots,” Nano Letters, **5** (5), 865–871 (2005)

[6] T. Ameri, G. Dennler, C. Lungenschmied and C. J. Brabec, “Organic tandem solar cells: A review,” Energy & Environmental Science, **2**, 347–363 (2009)

[7] G. Dennler, K. Forberich, T. Ameri, C. Waldauf, P. Denk, and C. J. Brabec, “Design of efficient organic tandem cells: On the interplay between molecular absorption and layer sequence,” Journal Of Applied Physics, **102**, 123109 (2007)

[8] L. Yang, H. Zhou, S. C. Price, and W. You, “Parallel-like Bulk Heterojunction Polymer Solar Cells,” Journal of American Chemical Society, Journal of the. American Chemical Society, **134** (12), pp 5432–5435 (2012)

[9] C. J. Brabec and J. R. Durrant, “Solution-Processed Organic Solar Cells,” Materials Research Society Bulletin, **33**, 670-675 (2008)

[10] J. Gilot, M. M. Wienk, and R. A. J. Janssen, “Optimizing Polymer Tandem Solar Cells,” Advanced Materials, **22**, E67–E71 (2010)

[11] Y. Yuan, J. Huang, and G. Li, “Intermediate Layers in Tandem Organic Solar Cells,” Green, **1**, 65–80 (2011)

[12] S. Cook, R. Katoh and A. Furube, “Ultrafast Studies of Charge Generation in PCBM:P3HT Blend Films following Excitation of the Fullerene PCBM,” Journal of Physical Chemistry, **113** (6), 2547–2552 (2009)

[13] A. Haugeneder, M. Neges, C. Kallinger, W. Spirkl, U. Lemmer, and J. Feldmann, “Exciton diffusion and dissociation in conjugated polymer/fullerene blends and heterostructures,” Physical Review B, **59** (23), 356-351 (1999)

[14] S. Isoda, “Energy Conversion Efficiency in Exciton Process for Single and Bulk Heterojunction Organic Solar Cells,” Journal of Applied Physics, **47**, 8859-8867 (2008)

[15] D. C. Olson, S. E. Shaheen, M. S. White, W. J. Mitchell, M. F. A. M. van Hest, R. T. Collins, D. S. Ginley, “Band-Offset Engineering for Enhanced Open-Circuit Voltage in Polymer–Oxide Hybrid Solar Cells,” **17** (2), 264–269 (2007)

[16] Z. M. Beiley, et al. “Morphology-Dependent Trap Formation in High Performance Polymer Bulk Heterojunction Solar Cells” Advanced Energy Materials **XX**, 1–9 (2011)

[17] M. Campoy-Quiles, et al. “Morphology evolution via self-organization and lateral and vertical diffusion in polymer:fullerene solar cell blends,” Nature Materials, **7** (2), 158-64 (2008)